A Novel Arabidopsis Vacuolar Glucose Exporter Is Involved in Cellular Sugar Homeostasis and Affects the Composition of Seed Storage Compounds[1][W][OA]

Gernot Poschet, Barbara Hannich, Sabine Raab, Isabel Jungkunz, Patrick A.W. Klemens, Stephan Krueger, Stefan Wic, H. Ekkehard Neuhaus, and Michael Büttner*

Centre for Organismal Studies, Ruprecht-Karls-University Heidelberg, D–69120 Heidelberg, Germany (G.P., M.B.); Molecular Plant Physiology, Friedrich-Alexander-Universität Erlangen-Nürnberg, D–91058 Erlangen, Germany (B.H., S.R., I.J.); Pflanzenphysiologie, Technische Universität Kaiserslautern, D–67653 Kaiserslautern, Germany (P.A.W.K., S.W., H.E.N.); and Biozentrum, Botanisches Institut II, Universität zu Köln, D–50674 Cologne, Germany (S.K.)

Subcellular sugar partitioning in plants is strongly regulated in response to developmental cues and changes in external conditions. Besides transitory starch, the vacuolar sugars represent a highly dynamic pool of instantly accessible metabolites that serve as energy source and osmoprotectant. Here, we present the molecular identification and functional characterization of the vacuolar glucose (Glc) exporter Arabidopsis (*Arabidopsis thaliana*) Early Responsive to Dehydration-Like6 (AtERDL6). We demonstrate tonoplast localization of AtERDL6 in plants. In Arabidopsis, *AtERDL6* expression is induced in response to factors that activate vacuolar Glc pools, like darkness, heat stress, and wounding. On the other hand, *AtERDL6* transcript levels drop during conditions that trigger Glc accumulation in the vacuole, like cold stress and external sugar supply. Accordingly, sugar analyses revealed that *Aterdl6* mutants have elevated vacuolar Glc levels and that Glc flux across the tonoplast is impaired under stress conditions. Interestingly, overexpressor lines indicated a very similar function for the ERDL6 ortholog Integral Membrane Protein from sugar beet (*Beta vulgaris*). *Aterdl6* mutant plants display increased sensitivity against external Glc, and mutant seeds exhibit a 10% increase in seed weight due to enhanced levels of seed sugars, proteins, and lipids. Our findings underline the importance of vacuolar Glc export during the regulation of cellular Glc homeostasis and the composition of seed reserves.

The transport of sugars across membrane barriers is essential for higher plants, because sugars represent transport and storage units of conserved energy and thus play a fundamental role during developmental processes and stress responses (Williams et al., 2000). The disaccharide Suc and the monosaccharide Glc are the most prominent soluble sugars in many plants and fulfill multiple functions in nutrition, signaling, and osmoregulation. In order to sustain proper development of nongreen sink tissues, plants have to distribute these sugars via long-distance transport, mostly in the form of Suc (Sauer, 2007; Dinant and Lemoine, 2010), which is taken up from the apoplast into sink cells directly or as its hydrolysis products Glc and Fru (Sherson et al., 2003; Büttner, 2007). In addition, sugars have to be distributed at the cellular level depending on the actual requirements. Within a cell, carbohydrates are stored in chloroplasts in the form of starch and in the vacuole as soluble sugars. While considerable effort has been expended in elucidating the flux of carbon in and out of the starch pool in chloroplasts (Zeeman et al., 2007), our current knowledge of carbon allocation in the vacuole and the corresponding transport steps is rather limited. However, understanding the details of vacuolar sugar partitioning is of major relevance, since several agriculturally important plants, like sugar beet (*Beta vulgaris*; Doll et al., 1979; Briskin et al., 1985; Getz, 1991; Getz and Klein, 1995) and sugarcane (*Saccharum officinarum*; Thom et al., 1982), accumulate considerable amounts of sugars in the vacuoles of storage organs.

The large central vacuole of a typical mesophyll cell can represent up to 90% of the total cell volume. It contains water, ions, enzymes, and a variety of primary and secondary metabolites and therefore fulfills vital functions, such as pH regulation, storage of essential ions, structural support, osmoregulation, and cell enlargement. Hence, vacuoles provide additional space for transient and long-term storage of sugars

[1] This work was supported by the Deutsche Forschungsgemeinschaft (grant nos. BU 973/7 to M.B. and FOR 1061 to M.B. and H.E.N.).

* Corresponding author; e-mail michael.buettner@cos.uni-heidelberg.de.

The author responsible for distribution of materials integral to the findings presented in this article in accordance with the policy described in the Instructions for Authors (www.plantphysiol.org) is: Michael Buettner (michael.buettner@cos.uni-heidelberg.de).

[W] The online version of this article contains Web-only data.

[OA] Open Access articles can be viewed online without a subscription.

www.plantphysiol.org/cgi/doi/10.1104/pp.111.186825

(Martinoia et al., 2007). In support of this aspect, several studies have provided biochemical evidence for the uptake of both Suc and hexoses into vacuoles (Thom et al., 1982; Rausch, 1991; Keller, 1992), and both passive diffusion and active transport have been determined as uptake mechanisms for these sugars (Thom and Komor, 1984; Martinoia et al., 1987, 2000). Furthermore, determination of subcellular sugar concentrations in a variety of plants via nonaqueous fractionation (Gerhardt and Heldt, 1984) revealed that in leaves, Glc is predominantly found in the vacuole, while Suc is mainly found in the cytosol or is evenly distributed (Wagner, 1979; Heineke et al., 1994; Pollock et al., 2000; Voitsekhovskaja et al., 2006).

In addition to the daily fluctuations due to photosynthetic activity, the vacuolar allocation of soluble sugars is also strongly influenced by stress factors like temperature changes, desiccation, and salt (Ingram and Bartels, 1996). Especially cold stress causes a strong increase of cellular Glc levels (Kaplan et al., 2004), and recently, this cold-induced accumulation of Glc was attributed to the vacuole (Wormit et al., 2006).

The passage of sugars across biomembranes is primarily mediated by transport proteins. The corresponding carriers for the uptake of Suc (Sauer, 2007) and hexoses (Büttner, 2010) across the plasma membrane have been identified and characterized for a variety of plants. In contrast, little is known about sugar transport proteins in the tonoplast. In sugar beet, a putative hexose transporter has been identified, and in vitro colocalization studies suggested vacuolar localization (Chiou and Bush, 1996), but evidence for transport activity was not provided. Only very recently, two previously unknown Glc transporter families, the tonoplast monosaccharide transporters (AtTMTs) and the vacuolar Glc transporters, have been identified in Arabidopsis (*Arabidopsis thaliana*), and direct or indirect transport assays support an import function for both types of transporters (Wormit et al., 2006; Aluri and Büttner, 2007). The activity of TMT limits seed yield in Arabidopsis (Wingenter et al., 2010) and is complex controlled by phosphorylation, catalyzed by a mitogen-activated protein triple kinase (Wingenter et al., 2011). However, Glc export from the vacuole, which was demonstrated biochemically, could not be attributed to one of the sugar transporters characterized so far.

Putative candidates for vacuolar Glc exporters might be found in the Arabidopsis *Early Responsive to Dehydration6-Like* (*AtERDL*) gene family, one of the least investigated subclades within the Arabidopsis Monosaccharide Transporter-Like (MST) family. The name for this subclade of the Arabidopsis MST family stems from ERD6 (At1g08930), a putative sugar transporter gene identified in a screening for genes responsive to dehydration or salinity stress (Kiyosue et al., 1998). For another member of this gene family, *ERD* (for *early response to dehydration*) *six-like1* (*ESL1*; At1g08920), vacuolar localization was demonstrated and heterologous expression in BY-2 cells of ESL1 mutant versions, which are mistargeted to the plasma membrane, gave the first hints for Glc transport activity (Yamada et al., 2010).

Here, we describe the molecular identification and functional characterization of a new vacuolar sugar transporter, AtERDL6 (At1g75220), which is located in the tonoplast and mediates Glc export from the vacuole, thereby regulating cellular Glc homeostasis in response to various stimuli and affecting the composition of seed storage reserves.

RESULTS

AtERDL6 Belongs to a Large Subclade of the Arabidopsis MST(-Like) Family, the ERD6-Like Genes

Annotation of genomic sequences from Arabidopsis identified *AtERDL6* as one of the 53 *AtMST* genes (Büttner, 2007). *AtERDL6* is localized on chromosome 1 (bacterial artificial chromosome F22H5.6; At1g75220), and computer analysis for splice site predictions (GENSCAN; NetGene2) and comparison with other *AtMSTs* suggested an *AtERDL6* coding sequence of 1,464 bp, interrupted by 16 putative introns. To verify this assignment, we amplified the *AtERDL6* open reading frame by reverse transcription (RT)-PCR and cloned the corresponding 1,472-bp PCR product into the vector pGEM-T Easy, yielding construct pSR6740u. Sequencing confirmed the predicted gene product and the number and positions of the 16 introns. *AtERDL6* encodes a 487-amino acid protein with a calculated molecular mass of 52,898 D and a pI of 8.73. Furthermore, the AtERDL6 protein sequence has 12 potential transmembrane regions, a feature characteristic for AtMSTs. According to the ProMEX database (Hummel et al., 2007), a Ser residue at position 32 or 33 can be phosphorylated. Notably, phylogenetic analysis revealed the existence of ERDL6 orthologs in all plant genomes sequenced to date, including dicots, monocots, gymnosperms, ferns, and mosses (Supplemental Fig. S1).

AtERDL6 Is Widely Expressed, Especially in Tissues with High Metabolic Turnover

First, the Genevestigator Arabidopsis Microarray Database and Analysis Toolbox (Eidgenössisch Technische Hochschule Zurich) was queried for plant-wide *AtERDL6* expression levels. According to these data sets, relatively high *AtERDL6* expression was found in many plant tissues and organs, including green tissues as well as nonphotosynthetic sink tissues at various developmental stages (Supplemental Fig. S2). In order to get a detailed picture of the *AtERDL6* expression profile during plant development and at the tissue level, we generated transgenic reporter plants expressing the GUS gene under the control of the *AtERDL6* promoter. Consistent with the microarray data, GUS reporter plants showed wide-

spread activity of the *AtERDL6* promoter in leaves, roots, and flower organs at various stages of development. In addition, these reporter lines allowed precise allocation of *AtERDL6* expression in various tissues, such as cotyledons, hypocotyls, and roots (except elongation zone) of seedlings and 3-week-old plants grown on petri dishes (already visible after 1 h of staining; Fig. 1, A–C), in all green leaves (rosettes, cauline leaves, and sepals; Fig. 1, D–H), in mature pollen grains and anther filaments (from flower stage 14; Fig. 1, G and J), in sepals (from flower stage 13; Fig. 1), in pedicels starting at flower stage 15 (Fig. 1G), in the abscission zone of flower leaves from flower stage 16 (Fig. 1G), and in seed pod walls (Fig. 1K).

Taken together, our analyses demonstrated a widespread pattern of *AtERDL6* expression especially pronounced in tissue types and developmental phases with high metabolic turnover, like seed germination, seedling establishment, pedicel and filament elongation, abscission, and wound response.

AtERDL6 Is a Transporter of the Vacuolar Membrane

Next, we determined the subcellular localization of AtERDL6 by transient expression of an *AtERDL6-GFP* fusion construct in Arabidopsis and tobacco (*Nicotiana benthamiana*). As depicted in Figure 2, Arabidopsis mesophyll protoplasts transiently expressing the *AtERDL6-GFP* fusion construct showed GFP fluorescence only in the tonoplast, clearly visible after protoplast lysis by mild osmotic shock as a ring with chloroplasts (red autofluorescence) attached at the outside (Fig. 2B). Additionally, tobacco leaves were infiltrated with an *Agrobacterium tumefaciens* culture harboring an *AtERDL6-GFP* fusion construct. Confocal sections of transformed epidermal cells showed GFP fluorescence of the vacuolar membrane that does not encompass chloroplasts (Fig. 2C). Furthermore, enzymatic removal of the cell wall and lysis of the protoplasts demonstrated that, also in tobacco, the AtERDL6-GFP fusion protein was clearly confined to the vacuolar membrane (Fig. 2D).

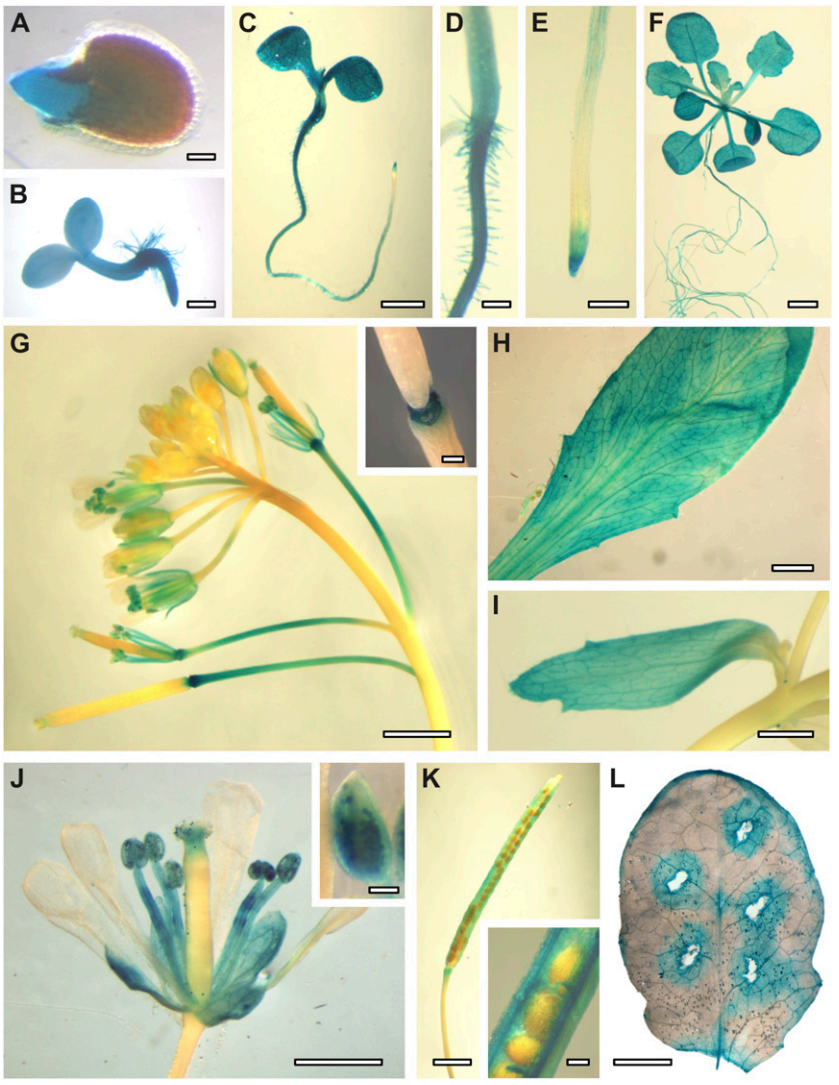

Figure 1. *AtERDL6* expression pattern. Histochemical localization of *AtERDL6* promoter-driven *GUS* expression is shown. A, Germinating seed with GUS activity in the emerging radicle. B, Two-day-old seedling with overall GUS expression. C to E, Five-day-old seedling with strong GUS staining in hypocotyl and cotyledons, root (except elongation zone), and root tip. F, Three-week-old plate-grown plant. G, Inflorescence and developing siliques. The inset shows an enlargement of the abscission zone of flower leaves and siliques. H, Mature rosette leaf. I, Cauline leaf. J, Flower with strong GUS staining in sepals, anthers, filaments, and pollen. K, Silique with GUS staining in seed pod walls. L, GUS activity in a mature leaf after wounding. In all experiments, GUS staining was stopped after 2 to 4 h and analyzed by light microscopy. Bars = 100 μm in A and J (inset), 200 μm in B, D, E, G (inset), K (inset), and L, 1 mm in C, I, and J, and 2 mm in F, G, H, and K.

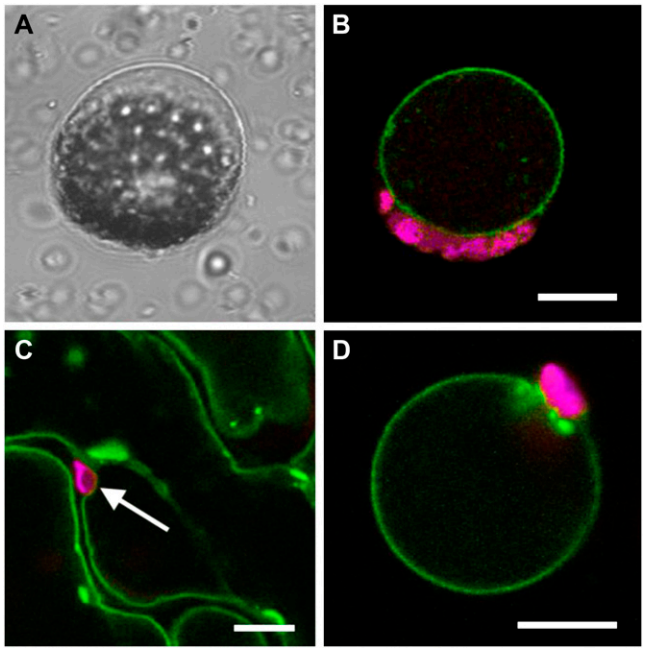

Figure 2. Tonoplast localization of the AtERDL6-GFP fusion protein in Arabidopsis and tobacco. Arabidopsis protoplasts (A and B) were transformed with an *AtERDL6-GFP* fusion construct. After 20 h of incubation, protoplasts were lysed by mild osmotic shock and analyzed by confocal laser scanning microscopy. A, Bright-field image of a protoplast after lysis, leaving the intact vacuole with attached chloroplasts. B, Fluorescence image of a lysed protoplast showing AtERDL6-GFP localization to the tonoplast (green) and chlorophyll autofluorescence (magenta) of attached chloroplasts. Tobacco leaves (C and D) were infiltrated with an *Agrobacterium* culture harboring the *AtERDL6-GFP* fusion construct pGP-67-1. After 2 d, infiltrated leaves were analyzed by confocal laser scanning microscopy. C, Epidermal leaf area depicting GFP fluorescence in tonoplasts of neighboring cells. D, Fluorescence image of a tobacco leaf protoplast after enzymatic degradation of the cell wall and lysis by mild osmotic shock, with GFP fluorescence restricted to the membrane of the remaining intact vacuole. Bars = 10 μm.

AtERDL6 Activity Affects Vacuolar Glc Levels

In order to examine the precise molecular function of the putative sugar transporter AtERDL6, we obtained two independent mutant lines, SAIL_528_F09 and SALK_106049, carrying T-DNA insertions at positions +2,262 (exon 12) and +3,139 (exon 17), respectively (Supplemental Fig. S3). Genomic PCR analyses verified homozygosity for the T-DNA alleles, and RT-PCR analyses confirmed the absence of full-length *AtERDL6* transcripts for both mutant lines (Supplemental Fig. S3).

Due to the demonstrated vacuolar localization of AtERDL6 and its homology to known MSTs, we examined the effect of the *erdl6* knockout on cellular sugar homeostasis. To this end, we quantified the content of soluble sugars in leaves from wild-type and *Aterdl6* mutant lines. As shown in Figure 3A, levels for Suc, Fru, and myoinositol were similar in the wild type and mutants. In contrast, a drastic increase by a factor of 2 was measured for the Glc content in both *Aterdl6* knockout lines (Fig. 3A).

In order to distinguish whether the lack of AtERDL6 affects whole cell Glc levels or results in vacuolar Glc accumulation, we determined sugar concentrations in subcellular compartments. Applying nonaqueous fractionation (Gerhardt and Heldt, 1984), we showed that the observed Glc increase in *Aterdl6* mutants was mainly due to an accumulation in the vacuole (398–402 ng mg^{-1} fresh weight in *Aterdl6* mutants and 140 ng mg^{-1} fresh weight in the wild type), while in the extravacuolar space, the difference in Glc levels was only marginal (32–34 ng mg^{-1} fresh weight in *Aterdl6* mutants and 22 ng mg^{-1} fresh weight in the wild type). Thus, in wild-type leaves, 86% of the total Glc is allocated to the vacuole, while in the *Aterdl6* mutants, the vacuolar Glc content accounts for 92% to 93% (Table I).

This increase of vacuolar Glc in plants lacking AtERDL6 strongly points toward an export function for this transporter. To further support this idea, we

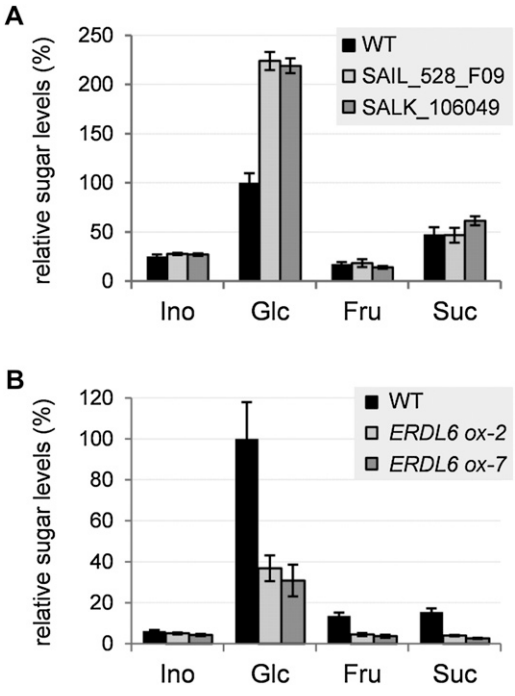

Figure 3. Changes of soluble sugar levels in leaves of *Aterdl6* mutant lines. Sugar content of unshaded leaves harvested 3 h after the onset of light was determined by HPAEC-PAD. Sugar levels relative to the wild-type (WT) Glc level are shown (100% equals 286 μg g^{-1} fresh weight in A and 574 μg g^{-1} fresh weight in B). A, Comparison of sugar levels in the wild type (black bars) and two independent *Aterdl6* mutant lines, SAIL_528_F09 (light gray bars) and SALK_106049 (dark gray bars). Plants were grown under short-day conditions for 3 weeks. *Aterdl6* mutant lines have a more than 2-fold increased Glc level. B, Comparison of sugar levels in the wild type (black bars) and two *AtERDL6*-overexpressing lines, ERDL6ox-2 (light gray bars) and ERDL6ox-7 (dark gray bars). Plants were grown under long-day conditions for 5 weeks. *AtERDL6* overexpressors show more than 50% reduction of the Glc level. For all experiments, data represent means ± SE of at least six biological replicates.

Table I. *Subcellular Glc distribution determined by nonaqueous fractionation and HPAEC-PAD*

Mature rosette leaves were assayed by nonaqueous fractionation according to Krueger et al. (2009). Values represent means ± SE of five biological replicates each for the wild type and mutant lines. Due to the much smaller volumes of chloroplasts and cytosol compared with vacuoles, the SD in these compartments is higher (Tilsner et al., 2005); thus, it was not possible to exactly determine whether the slightly elevated extravacuolar Glc levels are caused by changes in chloroplasts, the cytosol, or both.

Plant Line	Vacuolar Glc	Extravacuolar Glc
	ng mg^{-1} fresh wt	
Wild type	140 ± 20 (86%)	22 ± 3 (14%)
SALK_106049	409 ± 79 (92%)	34 ± 6 (8%)
SAIL_528_F09	398 ± 45 (93%)	32 ± 4 (7%)

generated transgenic plants overexpressing *AtERDL6* driven by the cauliflower mosaic virus (CaMV) *35S* promoter. In two independent transgenic lines with significantly increased *AtERDL6* transcript levels (11-fold in ERDL6ox-2 and 6-fold in ERDL6ox-7), soluble sugars were measured in leaves. In contrast to the elevated Glc levels found in *Aterdl6* knockout lines, plants overexpressing *AtERDL6* showed less than 50% of the wild-type Glc levels (Fig. 3B), further arguing for a Glc export function of AtERDL6. We also observed lower levels of Fru and Suc in the *AtERDL6*-overexpressing lines (Fig. 3B), suggesting an impairment of cytosolic sugar sensing/homeostasis due to excessive Glc export from the vacuole.

AtERDL6 Expression Is Regulated in Conditions That Require the Mobilization of Vacuolar Carbohydrate Stores

Knockout and overexpression of *AtERDL6* strongly influence vacuolar Glc allocation. Therefore, *AtERDL6* expression was monitored by quantitative RT-PCR under conditions that require the release of vacuolar Glc stores. First, we examined whether *AtERDL6* expression is regulated when photosynthesis is suppressed by darkness. When plants were kept in the dark for a short period (3 h) during the normal photoperiod, *AtERDL6* expression was induced by a factor of 3 (Fig. 4A). Moreover, a prolonged night with 24 h of darkness (instead of 8 h) led to a 5-fold induction of *AtERDL6* expression (Fig. 4A).

Conditions like heat stress and localized wound response also require instant availability and rapid release of cellular energy stores. Thus, we determined the *AtERDL6* expression level after temperature shift to 37°C or wounding of leaves. As shown in Figure 4, the *AtERDL6* expression in leaves increased dramatically after both treatments, about 3-fold after 6 h of heat stress at 37°C (Fig. 4B) and almost 7-fold 6 h after wounding (Fig. 4C), further supporting the function of the tonoplast transporter AtERDL6 in vacuolar Glc export.

We then addressed the question of whether *AtERDL6* expression is regulated by soluble sugars, which are a measure of the cellular energy status. Therefore, mature Arabidopsis leaves were incubated in 2% Glc, 2% Suc, or Murashige and Skoog (MS) medium without sugars, and the relative amounts of *AtERDL6* transcripts were determined by RT-PCR. As compared with the mock treatment, both Glc and Suc led to reductions of *AtERDL6* expression after 2 h of about 40% and 30%, respectively, which were still detectable after 6 h (Fig. 4D). Hence, *AtERDL6* expression is down-regulated by high external sugar concentrations, a condition where sugar release from the vacuole is not required.

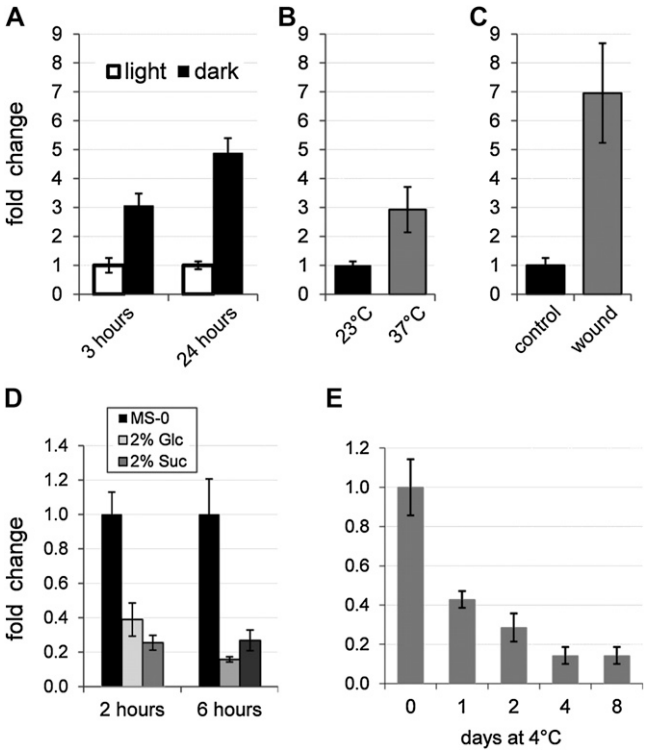

Figure 4. *AtERDL6* expression is significantly induced during darkness, heat stress, and wound response and down-regulated by sugars and cold stress. For all treatments, total RNA from 4-week-old rosette leaves was used to determine *AtERDL6* transcript levels by quantitative real-time PCR. A, Induction of *AtERDL6* expression after 3 and 24 h of darkness. B, Transcriptional induction by heat stress. Plants were incubated at normal (23°C) and elevated (37°C) temperatures for 6 h. C, Strong up-regulation of *AtERDL6* expression by wounding. Total RNA of wounded and unwounded leaves was extracted 6 h after treatment. D, Repression of *AtERDL6* expression by sugars. Leaves were incubated in liquid MS medium containing no sugars (black bars), 2% Glc (light gray bars), or 2% Suc (dark gray bars) for 2 or 6 h. E, Cold response of *AtERDL6*. Leaves were harvested 5 h after the onset of light before (day 0, 22°C) and during (1, 2, 4, and 8 d at 4°C) cold treatment. Shown are *AtERDL6* expression values relative to day 0 (no cold treatment). Data represent mean values ± SE of four independent biological replicates using *LDL3* (At4g16310) as a reference gene for A to D and of three independent experiments using *EF-1α* (At5g60390) as a reference gene for E.

It has previously been shown that several soluble sugars accumulate in vacuoles of Arabidopsis leaves upon exposure to low temperature (Wormit et al., 2006). In order to test if the application of cold stress also influences the expression level of the putative vacuolar Glc exporter AtERDL6, we determined *AtERDL6* transcript levels in plants that were transferred from normal temperature (22°C; day 0) to 4°C for 8 d. As shown in Figure 4E, already after 1 d, *AtERDL6* expression was reduced to about 40%, and it dropped continuously until a level of about 15% was reached at day 4, which remained constant for the rest of the sample period.

In summary, factors that affect vacuolar Glc allocation also influence *AtERDL6* transcript levels.

Aterdl6 Mutants Are Affected in Glc Export from the Vacuole Induced by External Signals

The impact of low temperature on vacuolar Glc accumulation and on *AtERDL6* expression prompted us to investigate the physiological consequences of the lack of AtERDL6 export function during the plant response to cold stress. Therefore, plants were kept at 4°C for 4 d to induce vacuolar Glc accumulation. Then, we transferred the plants to 22°C and compared the changes in Glc levels of wild-type and *Aterdl6* mutant plants during the period of rewarming, when Glc is released from the vacuole. In comparison with the wild type, the rate of Glc release from the vacuole was significantly slower in the *Aterdl6* mutants (Fig. 5A). While in wild-type plants, the Glc level dropped down to 37% after 7 h and to 16% after 14 h of rewarming, the *Aterdl6* mutants still had 57% to 58% and 40% to 41% of the initial Glc level after 7 and 14 h, respectively, indicating that a major route of Glc export from the vacuole is missing in *Aterdl6* mutants.

In contrast to the vacuolar Glc accumulation during cold stress, responses to elevated temperatures consume cellular energy and thus require the export of Glc from the vacuole. Accordingly, we found that *Aterdl6* mutants have a less marked mobilization of vacuolar Glc upon heat stress than wild-type plants. As seen in Figure 5B, wild-type plants reduced their Glc level to 39% after 6 h of heat stress, while mutants showed a reduction to only 62% to 71%. This difference was even more apparent when plants were kept in the dark during heat treatment. Under these conditions, wild-type plants reduced their Glc level to 27%, while mutants showed a reduction to only 44% to 46% (Fig. 5B).

Taken together, sugar measurements in *Aterdl6* mutants demonstrate that during adaptation to ambient temperatures, AtERDL6 is responsible for the export of a significant portion of Glc from the vacuole.

The ERDL6 Ortholog of Sugar Beet Also Mediates Glc Export When Expressed in Arabidopsis

Phylogenetic analyses revealed that ERDL6 orthologs are present in all plant genomes (Supplemental Fig. S1). Therefore, we investigated if an ERDL6-type transporter from another plant species also mediates Glc export from the vacuole. To this end, we used the previously identified cDNA clone (accession no. U43629, locus BVU43629) from sugar beet (Chiou and Bush, 1996) coding for Integral Membrane Protein (BvIMP), which is 80% identical and 92% similar to *AtERDL6*, for overexpression in Arabidopsis. U43629 transcript levels were monitored by northern-blot analysis, and two lines (lines 6 and 8) displaying

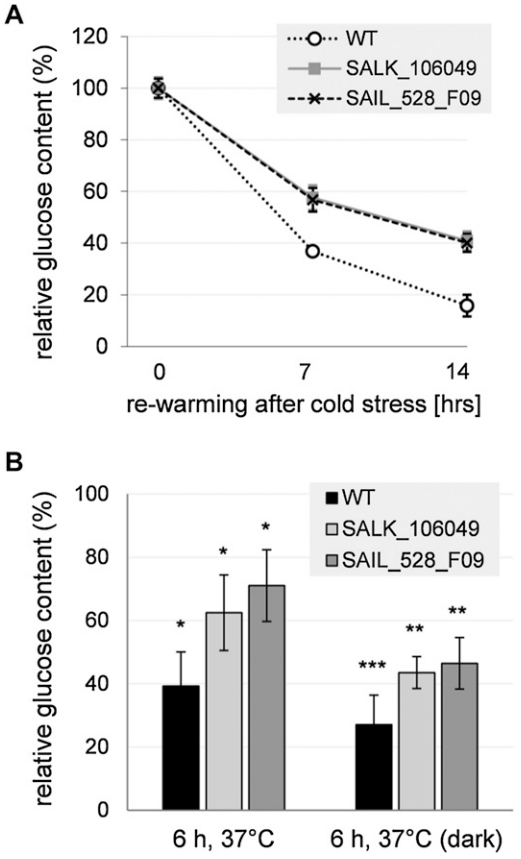

Figure 5. *Aterdl6* mutants show reduced Glc release from the vacuole in response to temperature changes. A, Cold stress response of *Aterdl6* mutants. The time course of Glc decrease in *Aterdl6* mutant leaves compared with the wild type (WT) is shown. Four-week-old plants were kept at 4°C for 2 d under long-day conditions to accumulate sugars in the vacuole. Upon transfer to 23°C, leaves were assayed for Glc content after 0, 7, and 14 h. Compared with the wild type (white circles), Glc decrease was significantly slower in mutants SALK_106049 (gray squares) and SAIL_528_F09 (black crosses), as indicated by changes relative to Glc levels at the end of the cold treatment (0 h). Data represent mean values ± SD of three biological replicates. B, Heat stress response of *Aterdl6* mutants. Four-week-old plants were incubated for 6 h at 37°C in the light or in darkness. For Glc quantification, leaf material was collected from unstressed plants 5 h after the onset of light and after 6 h of heat treatment. Shown are Glc levels relative to unstressed wild-type plants (100% equals 574 ± 74 ng mg^{-1} fresh weight). Data represent mean values ± SE of six biological replicates. Asterisks indicate significant differences from the untreated samples (*** $P < 0.001$, ** $P < 0.01$, * $P < 0.05$, as determined by Student's *t* test).

substantial expression of the *BvIMP* gene (Fig. 6A) were selected for further analysis. In order to measure the Glc levels in these overexpressor lines, we used seedlings grown in liquid culture (Wingenter et al., 2010). As shown in Figure 6B, both overexpressor lines showed significant decreases in Glc, representing about 66% to 69% of the wild-type level, similar to the transgenic lines overexpressing *AtERDL6* (Fig. 3B). Cold treatment induces Glc relocation into the vacuole, as previously demonstrated. Therefore, we wanted to test if lines overexpressing the sugar beet cDNA show differences in Glc release during rewarming after cold incubation. Five- to 6-week-old plants were kept at 4°C for 3 d and then transferred to 22°C at the beginning of the dark phase. As seen in Figure 6C, in wild-type plants, the level of Glc dropped to 65% and 35% after 7 and 14 h, respectively, demonstrating release and metabolization of Glc, which previously accumulated in the vacuole during the cold treatment. However, lines expressing *BvIMP* displayed a more pronounced Glc release, indicated by the lower Glc levels being only 44% and 17% (of the initial value) after 7 and 14 h, respectively (Fig. 6C). This difference strongly suggests a stimulated Glc export capacity at the tonoplast in these lines. No differences between the wild type and overexpressors were observed for the release of Suc, which also accumulates during the cold (data not shown). Consistent with the proposed export function, *BvIMP* overexpression resulted in the opposite effect as observed for the *Aterdl6* mutant lines (Fig. 5A), namely, a faster decrease in cellular Glc levels due to a more rapid release from the vacuole.

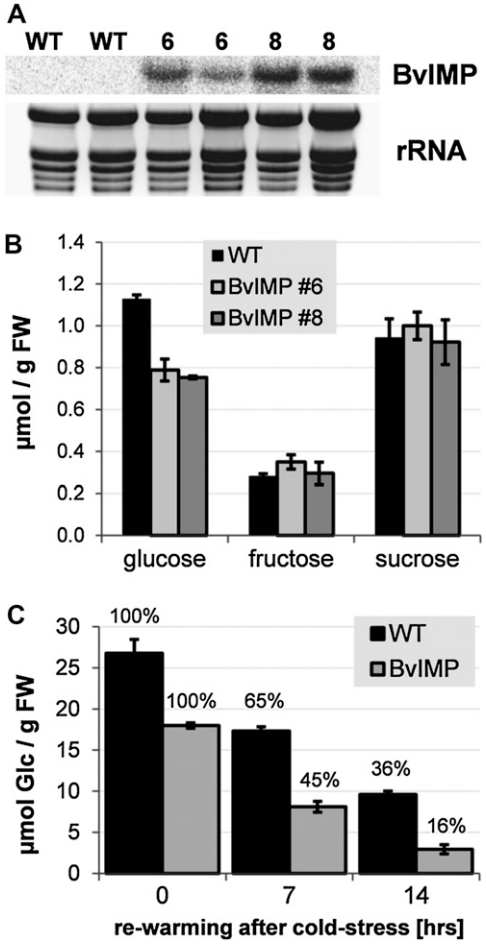

Figure 6. Overexpression in Arabidopsis of the AtERDL6 ortholog *BvIMP* supports the Glc export function from the vacuole. A, Northern-blot analysis of Arabidopsis lines 6 and 8 overexpressing the sugar beet clone U43629, coding for BvIMP. Total RNA was isolated from 5-week-old plants; rRNA represents the loading control. B, Glc levels in the wild type (WT) and *BvIMP*-overexpressing lines grown in liquid culture. Wild-type plants (black bars) and *BvIMP*-overexpressing lines 6 (light gray bars) and 8 (dark gray bars) were grown in standard liquid culture medium for 12 d. Each data point represents the mean value of three independent biological experiments ± SE. C, Release of Glc after cold-induced accumulation in the vacuole. Both the wild type (black bars) and *BvIMP*-overexpressing line 6 (light gray bars) were incubated for 3 d at 4°C under long-day conditions and transferred to 22°C for rewarming after the start of the dark phase (0 h) at day 3. Leaf Glc contents were quantified by ion chromatography. Each data point represents the mean value of three independent biological experiments ± SE. FW, Fresh weight.

Lack of AtERDL6 Export Activity Causes a Delay of Seed Germination in the Presence of Glc

Since our GUS reporter plants demonstrated a high expression level of *AtERDL6* in germinating seeds (Fig. 1A), we examined the *Aterdl6* mutants for detectable changes during this vital developmental process. While germination rates of mutant and wild-type seeds were nearly identical on 2% sorbitol and 2% Suc (data not shown), *Aterdl6* seed germination was significantly delayed with increasing amounts of Glc in the growth medium (Fig. 7). In the absence of sugars, wild-type seeds started to germinate when incubated for 2 d in light (DIL) and reached 40% germination at 3 DIL (Fig. 7, top panel). It has been shown before that Glc delays seed germination in Arabidopsis (Dekkers et al., 2004). Accordingly, 2% Glc in the growth medium slightly delayed wild-type seed germination, reaching 70% at 4 DIL (Fig. 7, middle panel). This delay was even more pronounced in the presence of 7.2% Glc, where 50% germination was reached only at 7 DIL (Fig. 7, bottom panel). This negative effect of Glc on seed germination was much more pronounced in *Aterdl6* mutant lines. With 2% Glc, 50% germination was detected between 5 and 6 DIL (about 2 d later than in the wild type), and with 7.2% Glc, 50% germination was reached only after 12 DIL (more than 5 d later than in the wild type).

Aterdl6 Mutants Show a Significant Elevation of the Major Seed Storage Compounds

Due to the observed difference in seed germination, we also analyzed seed sugar composition as well as protein and lipid content in *Aterdl6* mutant lines. As shown in Table II, mutant lines contain more than

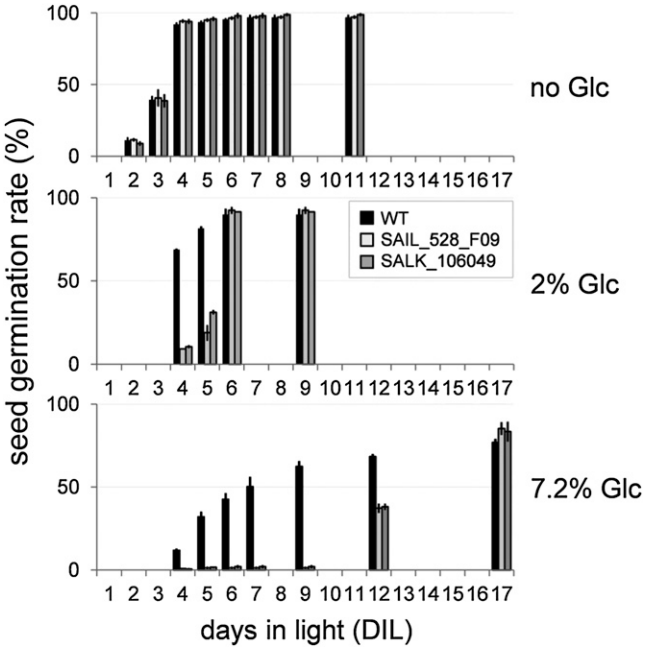

Figure 7. *Aterdl6* mutant seeds display enhanced sensitivity to external Glc during seed germination. Wild-type (WT) and *Aterdl6* mutant seeds were germinated on MS plates containing no sugar, 2% Glc, and 7.2% Glc. Glc reduces the germination rate of wild-type seeds (black bars). However, a further delay can be seen with seeds of mutant lines SAIL_528_F09 (light gray bars) and SALK_106049 (dark gray bars) germinating in the presence of 2% Glc, which is even more prominent with 7.2% Glc. Data represent mean values ± SE of three replicate experiments with 80 to 140 seeds per line.

double the amount of Glc compared with the wild type, whereas the amount of Suc was unchanged. Further analyses of the mutant seeds revealed that the total protein content is increased by more than 50% and also that the lipid content is more than 10% higher than in the wild type. Most interestingly, as a consequence of elevated soluble sugars, proteins, and lipids, the *Aterdl6* mutant seed weight is increased significantly, as determined by the "thousand seed weight" being 16.7 ± 0.6 mg for the wild type and 18.4 ± 0.4 and 18.5 ± 0.4 mg for the mutant lines SAIL_528_F09 and SALK_106049, respectively (Table II). Moreover, this increase in single seed weight is not at the expense of total seed quantity, as shown by the nearly unchanged number of seeds per silique (61.2 ± 1.2 in the wild type versus about 63 ± 1.2 in the mutant lines) and the total seed weight per plant (191 ± 16 in the wild type versus 222 ± 16 and 223 ± 14 in the mutant lines). Thus, the total seed yield per plant is increased by more than 10% in the *Aterdl6* mutant lines (Table II).

DISCUSSION

Sugars have essential functions in a number of plant cellular processes, including storage units of energy and building of structural components and signal molecules. Therefore, metabolic conversion, storage, and compartmentalization have to be tightly regulated, which often requires the transport of sugars across biomembranes. Consequently, plant genomes contain a great number of genes coding for sugar transport proteins, which sometimes form large families according to their specific functions as determined by substrate specificity, subcellular localization, and/or transport mechanism (Büttner, 2007; Sauer, 2007). While numerous transport proteins that import sugars into cells and cellular compartments have been identified to date, little effort has been devoted to identifying transporters that mediate sugar flux in the opposite direction, out of cells or organelles.

In this paper, we present the molecular identification and functional characterization of a previously unknown vacuolar Glc exporter, AtERDL6. A survey of public plant sequence databases revealed that genes coding for ERD6-like transporters exist in all plant genomes sequenced so far, including higher plants, ferns, and mosses (Supplemental Fig. S1), underlining a fundamental function of this type of sugar transporter.

Analysis of GUS reporter plants revealed a widespread expression pattern of *AtERDL6* (Fig. 1) that was particularly prominent in tissues and developmental phases with high metabolic turnover, which included germinating seeds, young seedlings, elongating ped-

Table II. *Seed sugar composition, protein and lipid content, and seed weight in Aterdl6 mutants*

Values refer to the dry weight of mature seeds and represent means ± SE of biological replicates. Independent experiments were performed for the analysis of sugars ($n = 4$), proteins ($n = 5$), lipids ($n = 3$), thousand seed weight ($n = 8$), seeds per silique ($n = 18$), and seed weight per plant ($n = 7$). Percentages given in parentheses are relative to the corresponding wild-type values, which were set to 100%.

Parameter	Wild Type		SAIL_528_F09		SALK_106049	
Sugars (μg mg^{-1} dry wt)						
Glc	0.45 ± 0.07	(100%)	1.04 ± 0.04	(231%)	1.40 ± 0.10	(311%)
Suc	2.74 ± 0.05	(100%)	2.72 ± 0.04	(99%)	2.55 ± 0.12	(93%)
Proteins (μg mg^{-1} dry wt)	158 ± 24	(100%)	241 ± 16	(154%)	243 ± 21	(152%)
Lipids (μg mg^{-1} dry wt)	240 ± 5	(100%)	284 ± 29	(119%)	270 ± 30	(113%)
Thousand seed weight (mg)	16.7 ± 0.6	(100%)	18.4 ± 0.4	(110%)	18.5 ± 0.4	(111%)
Seeds per silique	61.2 ± 1.2	(100%)	63.5 ± 1.2	(104%)	63.1 ± 1.1	(103%)
Seed weight per plant (mg)	191 ± 16	(100%)	222 ± 16	(116%)	223 ± 14	(117%)

icels and filaments, programmed and induced cell death in abscission zones, and wounded tissues. Our results are supported by *AtERDL6* expression data found in public microarray databases (Supplemental Fig. S2) and indicate a role of this new sugar transporter in cellular carbon distribution. Localization of a translational GFP fusion clearly assigned AtERDL6 to the tonoplast in Arabidopsis and tobacco (Fig. 2). This finding is in agreement with results from a recent proteome study, where AtERDL6 was identified in the vacuolar fraction (Jaquinod et al., 2007).

AtERDL6 Regulates Cellular Glc Homeostasis in Response to Several Environmental Factors

In support of a role in Glc export from the vacuole, we found a strong transcriptional regulation of *AtERDL6* expression in response to conditions that alter cellular sugar levels and require the activation of cellular carbohydrate stores. It is long known that exposure to drastic temperature changes induces profound adaptations in carbon metabolism (Ristic and Ashworth, 1993). In Arabidopsis, cold stress at 4°C leads to a drastic increase in soluble sugar levels within the first 12 h (Kaplan et al., 2004). A similar effect on primary metabolism is also seen under heat stress, although cold stress appears to cause a more dramatic metabolic response (Shulaev et al., 2008). However, while Suc (and many other soluble sugars like Fru, maltose, and raffinose) accumulates under both temperature treatments, Glc is accumulating in the cold but is decreasing under heat stress (Kaplan et al., 2004). It is discussed that Glc is released from the vacuole to sustain Suc production in the cytosol, which in turn serves as an osmoprotectant in maintaining cell membrane integrity and cellular function under stress (Ruan et al., 2010). We determined *AtERDL6* expression levels under both temperature stress conditions. In line with its Glc export function, cold stress, which causes Glc accumulation in the vacuole, strongly represses *AtERDL6* (Fig. 4E). Interestingly, the closely related *AtERD6* gene (At1g08930) shows an opposite regulation and is induced during cold stress (Kiyosue et al., 1998). This might indicate different functions within the ERD6-like transporter family with respect to substrates and transport direction. In contrast to its cold repression, we found a strong *AtERDL6* induction when plants were exposed to elevated temperatures and consumed Glc (Fig. 4C), coinciding with the decrease in cellular Glc levels under these conditions.

Wounding induces a wide number of cellular responses, including respiration, cell division, and biosynthesis of secondary metabolites. Sealing wound sites and repairing damaged tissues requires metabolic energy provided by pools of soluble sugars (Roberts and de Bruxelles, 2001). We found that wounding triggered a more than 7-fold increase of *AtERDL6* expression (Fig. 4C). Interestingly, treatment with methyl jasmonate, a phytohormone regulating the plant's response to wounding, pathogen attack, and other stress conditions, also elicits a strong increase in *AtERDL6* expression (1 h, 2.2-fold; 3 h, 3.5-fold; NASCARRAYS-174).

Another condition that requires access to cellular energy stores is darkness. At the light-to-dark transition and during the night, transitory starch represents the main pool of stored energy. However, vacuolar Glc also can serve the same purpose, especially for immediate compensation of photosynthesis switch off. We measured *AtERDL6* transcript abundance after a 3-h dark period interrupting the normal light cycle during the day as well as after a prolonged night. Both conditions of "light starvation" led to a strong induction of *AtERDL6* expression (Fig. 4A).

Since we could not distinguish whether the observed dark induction is a direct effect of the absence of light or is indirectly mediated by the drop in photosynthetic products, we tested the effect of sugars on *AtERDL6* expression. We could measure a downregulation of *AtERDL6* by feeding leaves with the primary metabolites Glc and Suc (Fig. 5), indicating that AtERDL6-mediated Glc export from the vacuole is controlled via sugar signaling. Consistent with this finding, a significant regulation of *AtERDL6* by sugars was also found in transgenic plants with mutations related to sugar metabolism. The *pho3* mutant, which harbors a defective copy of the Suc transporter *SUC2* gene, accumulates large amounts of soluble sugars. In this mutant, *AtERDL6* transcript levels are reduced to about 50% (Lloyd and Zakhleniuk, 2004). The Snf1-related protein kinase AKIN10 controls reprogramming of transcription in response to darkness, sugar, and stress conditions. Transgenic AKIN10 overexpression, which confers enhanced starvation tolerance (Baena-González et al., 2007), triggers a 2.5-fold increase of *AtERDL6* expression (Gene Expression Omnibus series GSE8257), which in turn enhances the availability of vacuolar Glc. Finally, in independent studies investigating the effect of Glc treatment on the transcriptome level, *AtERDL6* expression is markedly affected. Price et al. (2004) found a more than 5-fold reduction by 3% Glc, which was not seen with the nonmetabolizable analog 3-*O*-methylglucose. Similarly, Li et al. (2006) reported 4- and 5-fold reductions after treatment with 3% Glc for 2 and 6 h, respectively, which could not be observed with 3% mannitol. Interestingly, also the grapevine (*Vitis vinifera*) monosaccharide transporter VvHT1 was shown to be regulated by Glc at both the transcriptional and posttranscriptional levels (Conde et al., 2006).

In conclusion, our studies on *AtERDL6* transcriptional regulation revealed a strong responsiveness to changes in the cellular sugar status that require instant access to vacuolar sugar pools.

Physiological Role of the Vacuolar Glc Exporter AtERDL6

To verify the role of AtERDL6 as a vacuolar Glc exporter in planta, we have chosen a reverse genetics

approach and isolated two independent mutant lines, SAIL_528_F09 and SALK_106049, in which *AtERDL6* expression was absent (Supplemental Fig. S2). Analysis of cellular sugar levels revealed that while most of the common sugars were not affected in the *Aterdl6* mutants, a clear increase in cellular Glc levels was detectable, indicating that in the mutants a transport activity at the tonoplast is missing, which traps Glc within the vacuole. Moreover, nonaqueous fractionation clearly demonstrated that, in contrast to wild-type leaves, which allocate 86% of the total Glc in the vacuole, in *Aterdl6* mutant leaves, 92% to 93% of the total Glc is found in the vacuole (Table I). Consistent with AtERDL6-driven Glc export from the vacuole, we found markedly decreased Glc levels in *AtERDL6*-overexpressing lines (Fig. 3B). However, we also observed lower levels of Fru and Suc in these overexpressor lines (Fig. 3B). It is unlikely that AtERDL6 also directly mediates the export of Fru and Suc, since we could not measure an accumulation of these sugars in *Aterdl6* knockout plants. It seems more likely that the excessive export of Glc from the vacuole alters cytosolic Glc signaling/homeostasis and thus indirectly affects Fru and Suc levels. To further substantiate our model of AtERDL6-driven Glc export from the vacuole, we analyzed the sugar levels in mutant lines exposed to cold stress that was shown to affect *AtERDL6* expression. Since Glc accumulates in the vacuole during cold treatment, we expected an effect on Glc release from the vacuole during rewarming of the plants. In fact, both *Aterdl6* mutant lines displayed significantly slower reductions of cellular Glc levels as compared with the wild type, which can be attributed to less efficient export from the vacuole (Fig. 5A). Similarly, upon heat stress (and even more obviously in combination with darkness), the liberation of the vacuolar Glc pool was significantly slower in the *Aterdl6* mutants as compared with the wild type (Fig. 5B). The fact that in *Aterdl6* mutants, Glc export from the vacuole is not completely absent is most likely due to one (or more) of the 18 other members of the *AtERDL6* gene family, some of which show partial overlap in their expression patterns, according to public microarray data sets (Genevestigator).

Finally, we also addressed the physiological function of the AtERDL6 ortholog BvIMP from sugar beet. *BvIMP* overexpression in Arabidopsis resulted in a similar decrease of cellular Glc levels as observed for *AtERD6* overexpressors. In addition, when *BvIMP* overexpressors were subjected to low temperatures in order to induce vacuolar Glc accumulation and subsequently brought back to normal growth temperatures, the cellular Glc levels dropped significantly faster as compared with wild-type plants, indicating a faster Glc release from the vacuole during rewarming due to additional export capacity (Fig. 6).

All our results are in line with an export activity for AtERDL6 mediating Glc transport from the vacuole to the cytosol, and a lack of this transport step results in significant accumulation of Glc in the vacuole. However, *Aterdl6* mutant lines developed completely normally and were indistinguishable from the wild type under standard growth conditions as well as after application of stress conditions like cold shock, drought, or salt stress (data not shown). Since *AtERDL6* transcript levels are relatively high in mature seeds (NASCARRAYS-69, NASCARRAYS-183, NASCARRAYS-195, NASCARRAYS-497; Gene Expression Omnibus series GSE15700), we examined the impact of different sugars on seed germination. Interestingly, with increasing amounts of Glc in the medium, the seed germination rate was significantly delayed (Fig. 7). This effect could not be detected with comparable amounts of Suc or sorbitol (as osmoticum), indicating the involvement of a Glc-specific signaling pathway.

Several recent studies revealed a negative influence of external Glc on seed germination. The production of sugars from starch is inhibited by increasing sugar levels in germinating cereal seeds by the repression of α-amylases (Karrer and Rodriguez, 1992). In germinating Arabidopsis seeds, the presence of exogenous Glc significantly retards the mobilization of seed storage lipid (To et al., 2002). Dekkers et al. (2004) have shown that Glc acts on embryo growth and that the inhibition of seed germination is independent of hexokinase function. Furthermore, exogenous Glc blocks seed germination by delaying the decline in endogenous abscisic acid concentration (Price et al., 2003). Thus, if germinating on high external Glc concentrations, seeds might sequester excess Glc from the cytosol into the vacuole to avoid these negative effects via Glc signaling. However, the vacuolar buffering capacity for Glc might be exhausted in *Aterdl6* mutants, which already have a constantly elevated Glc level in the vacuole and, therefore, are more susceptible to external Glc, which then causes the observed delay in seed germination.

Due to the higher Glc sensitivity during seed germination, we have analyzed *Aterdl6* mutant seeds in more detail and found that the major seed storage compounds were elevated (i.e. Glc by more than 100%, proteins by 53%, and lipids by 10%), while Suc was unchanged. This rise in storage compound deposition also led to an increase in single seed weight and total seed yield per plant of about 10% (Table II). This is in perfect agreement with the effect that was observed after overexpressing the tonoplast monosaccharide importer TMT1 (Wingenter et al., 2010), which also led to a significant increase of vacuolar Glc levels as well as lipids and proteins, causing a seed weight gain similar to that in *Aterdl6* knockouts. Further analyses will be needed to show if the increase in Glc, proteins, and lipids in *Aterdl6* mutants is balanced by a compensatory decrease of other components (e.g. secondary metabolites).

In summary, this paper presents the characterization of the vacuolar Glc exporter AtERDL6, which localizes to the tonoplast and is transcriptionally regulated by a number of internal and external factors that entail vacuolar partitioning of Glc. Lack of AtERDL6 causes

significant increases in vacuolar Glc levels and negatively affects the release of vacuolar Glc during the heat stress response and during a rewarming phase after a cold period. Our findings underpin the important role of vacuolar Glc export during the regulation of cellular Glc homeostasis and the composition of seed reserves.

MATERIALS AND METHODS

Strains and Growth Conditions

Escherichia coli strain DH5α (Hanahan, 1983) was used for cloning. Arabidopsis (*Arabidopsis thaliana*) ecotype Columbia was grown in potting soil in the greenhouse or on agar medium in growth chambers at 22°C and 55% relative humidity under short-day (8 h of light/16 h of dark) or long-day (16 h of light/8 h of dark) conditions, as indicated. Arabidopsis transformation was performed with *Agrobacterium tumefaciens* strain GV3101 (Holsters et al., 1980) using the floral dip method (Clough and Bent, 1998).

Cloning of the *AtERDL6* cDNA

The full-length *AtERDL6* cDNA (GenBank accession no. AY124845) was obtained using gene-specific primers AtERD67g-10f_BspHI (5′-GAATCAAATCATGAGTTTCAGGGATGATAATGA-3′) and AtERD67c+1462r_BspHI (5′-CGCGTCATGAATCTGAACAAGGATTGAAGTTCTTC-3′) and total RNA from leaves to amplify the *AtERDL6* open reading frame by RT-PCR. The corresponding 1,472-bp PCR product was cloned into pGEM-T Easy and sequenced, yielding pSR6740u.

Generation of *AtERDL6* Promoter/GUS Lines and Histochemical Localization of GUS Activity

In order to generate *AtERDL6* promoter/GUS plants, a 2-kb fragment upstream of the *AtERDL6* coding region was amplified by PCR using primers ERD67g-2056f_*Pst*I (5′-GATCTTGGTAGCTGCAGACGATACATTGC-3′) and ERD67g+16r_*Nco*I (5′-CATCCCTGAAACCCATGGTTTGATTCTATC-3′) and genomic DNA, cloned into pGEM-T Easy, and sequenced, yielding pSR6730. From here, the promoter fragment was cloned via *Pst*I and *Nco*I sites into pSR1, a pUC19-based plasmid harboring the *GUS* reporter gene, yielding pSR6721. A *Pst*I/*Sac*I fragment containing the *AtERDL6* promoter, the GUS reporter gene, and the *Nos* terminator was transferred to pGBTV-bar (Becker et al., 1992), yielding construct pSR6722. *Agrobacterium*-mediated transformation of Arabidopsis (floral dip) produced 30 independent transgenic lines that were analyzed for GUS activity in the T1 and T2 generations.

Subcellular Localization of AtERDL6

To determine the compartment to which AtERDL6 is targeted within the cell, we cloned the *AtERDL6* cDNA from pSR6740u into pSO35e, a pUC19-based plasmid harboring the *GFP* reporter gene (Aluri and Büttner, 2007) via *Bsp*HI sites. The resulting construct, pSR6760, was used for transient expression in Arabidopsis mesophyll protoplasts as described (Aluri and Büttner, 2007), and *AtERDL6-GFP* expression was monitored by fluorescence microscopy. In addition, an AtERDL6-GFP fusion construct was transiently expressed in tobacco (*Nicotiana benthamiana*) by leaf infiltration. To this end, the *AtERDL6* cDNA was amplified by PCR using *AtERDL6*-specific primers AtERD67c+1f GW (5′-CACCATGAGTTTCAGGGATGATAATGAGGAGGC-3′) and AtERD67c +1461r-STOP (5′-TCTGAACAAGGATTGAAGTTCTTCAAGAGTT-3′) and leaf cDNA as template and then cloned into pENTR/D-TOPO (Invitrogen). To generate the construct for subcellular localization, a Gateway LR reaction was performed transferring the *AtERDL6* coding sequence into the destination vector pK7FGW2.0 (Karimi et al., 2002) in front of the GFP sequence, yielding vector pGP67-1. For transient transformation, tobacco leaves were infiltrated with an *Agrobacterium* culture (strain C58C1; Deblaere et al., 1985) harboring pGP-67-1 and analyzed after 2 d by confocal laser scanning microscopy. To obtain tobacco protoplasts, leaves were gently roughened with sandpaper 2 d after infiltration and incubated for 1 h at 30°C in an enzymatic mix containing 0.5% Cellulase Onozuka R-10 (Serva), 0.05% Pectolyase Y-23 (Sigma-Aldrich), 1% bovine serum albumin, 10 mM MES, pH 5.5, and 600 mM sorbitol.

Generation of *AtERDL6* and *BvIMP* Overexpressor Mutants

To generate an *AtERDL6* overexpressor construct, we used a modified version of the plant vector pGPTV-bar (Becker et al., 1992). To this end, the *Eco*RI site was removed by restriction digestion following a nucleotide fill-in reaction and religation, yielding vector pRG1. An 814-bp *Hin*dIII/*Xma*I fragment from pSO35e (Aluri and Büttner, 2007) containing the enhanced CaMV *35S* promoter was inserted into pRG1 digested with *Hin*dIII and *Xma*I, yielding pRG3. Restriction digestion of pRG3 with *Sac*I removed the GUS reporter fragment, and insertion of a linker [annealed oligonucleotides ESS-linker(+), GAATTCCTGCAGGAGCT, and ESS-linker(−), CCTGCAGGAATTCAGCT] introduced a new *Eco*RI site behind the CaMV *35S* promoter in the new vector pRG5. The *AtERDL6* cDNA was PCR amplified using primers AtERD67c-21f_*Eco*RI (5′-AATTCAAGCTTGTAAAAGAAATGAGTTTCAGGGATGATAATG-3′) and AtERD67c+1464r_*Sac*I (5′-GAGCTCATCTGAACAAGGATTGAAGTTCTTC-3′) and cloned into pRG5 digested with *Eco*RI and *Sac*I in two consecutive steps due to the internal *Eco*RI site of the *AtERDL6* coding sequence, yielding construct pSR6772. *Agrobacterium*-mediated transformation of Arabidopsis (floral dip) produced 25 independent transgenic lines that were analyzed for *AtERDL6* expression by RT-PCR, identifying ERDL6ox-2 and ERDL6ox-7 as strong overexpressor lines, with 11- and 6-fold increased *AtERDL6* expression levels, respectively. *BvIMP* overexpressors were generated by amplifying the *U43629* cDNA via PCR using primers BvIMP-for_*Xho*I (5′-TTTCTCGAGATGAGTTCAGATTCAGAAGC-3′) and BvIMP-rev_*Hin*dIII (5′-TTTAAGCTTTTATCTTCTGAAGGACC-3′). The product was inserted into pBSK (digested with *Eco*RV), excised by using *Xho*I and *Hin*dIII, and further cloned into the correspondingly digested pHannibal vector. Thereafter, the construct was digested with *Not*I and cloned into the correspondingly treated pART27 vector. Transformation of Arabidopsis by *Agrobacterium*-mediated floral dip generated eight independent transgenic overexpressor lines, of which lines 6 and 8 were identified as the strongest by northern-blot analysis.

Plant Treatments for *AtERDL6* Expression Analyses

To analyze the effect of darkness and external sugars on *AtERDL6* expression, plants were treated as described (Poschet et al., 2010). For heat stress experiments, plants were wrapped in aluminum foil to prevent dehydration and incubated for 6 h at 37°C (stress) or 23°C (control) in an incubator (Binder). To determine the impact of wounding, leaves were pinched with a syringe in a homogenous pattern. Leaves of unwounded plants as well as unwounded leaves from treated plants served as controls. Total RNA was extracted after 6 h. To determine the cold stress response of *AtERDL6*, plants were kept for 1 week at 4°C. RNA was prepared from leaves harvested 5 h after the beginning of the light phase before (day 0, 22°C) and during (days 1, 2, 4, and 8) cold treatment.

RNA Isolation and Quantitative Real-Time PCR Analysis

Total RNA was isolated as described (Schneidereit et al., 2003), and RT-PCR was performed according to the supplier's instructions (MBI Fermentas). Primers AtERD67c+1068fRT (5′-TCGGTTGGGATGACGATTAGCC-3′) and AtERD67c+1199rRT (5′-TGGTCCCATTCCCAATGAGAAAAAG-3′) were used to PCR amplify *AtERDL6*-specific products from the indicated tissues. In parallel, primers AtLDL3-fRT (5′-TACTGGTAAACAGAGGCAGAAACA-3′) and AtLDL3-rRT (5′-TTCTTGTTACCCTTCAACCTCTTC-3′) were used to amplify the *LDL3* transcript as a reference (Czechowski et al., 2005). PCRs contained 0.2 μL of cDNA, 0.5 μM of each primer as indicated, and 2× Maxima SYBR Green/ROX qPCR Master Mix (Fermentas), and PCR amplification was performed in a RotorGene 2000 system (Corbett Research). Relative transcript abundance was determined using the comparative $\Delta\Delta C_T$ method (Livak and Schmittgen, 2001) with the RotorGene software version 5.

Plant Treatments for Sugar Analyses

To determine the effect of heat stress and/or dark incubation on soluble sugar content in leaves, wild-type and *Aterdl6* mutant plants were treated as described for RT-PCR analyses.

To quantify sugar levels during the rewarming phase after cold treatment, plants were kept at 4°C for 3 d. Thereafter, plants were transferred back to standard growth temperature (22°C) at the beginning of the night phase and

kept in the dark. Leaves were harvested 0, 7, and 14 h after cold treatment and subjected to sugar analysis by ion chromatography.

Sugar Quantification by Ion Chromatography

Soluble sugars were extracted from plant material with 80% ethanol for 1 h at 80°C and quantified by high-performance anion-exchange chromatography with pulsed amperometric detection (HPAEC-PAD) in an ICS-3000 system (Dionex) with a CarboPac PA1 column and 15 to 300 mM NaOH (Fluka) in HPLC-water (VWR) as eluent. Quantitative calculation of sugars was performed using Chromeleon software 6.7 (Dionex).

Identification of T-DNA-Tagged Arabidopsis Knockout Lines for *AtERDL6*

Line SAIL_528_F09 (insertion at position +2,284, exon 12) was obtained from the Torrey Mesa Research Institute. Line SALK_106049 (insertion at position +3,107, exon 17) was obtained from the T-DNA mutant collection at the Salk Institute and provided by the Nottingham Arabidopsis Stock Centre (http://nasc.nott.ac.uk/). Plants homozygous for both *Aterdl6* alleles were identified by PCR with genomic DNA and primers flanking the insertion site. In addition, the absence of *AtERDL6* transcript in these knockout lines was verified by RT-PCR analyses with total RNA and *AtERDL6*-specific primers spanning the insertion site: AtERD67g-10f_BspHI (5′-GAATCAAATCATGAGTTTCAGGGATGA-TAATGA-3′) and AtERD67c+1462r_BspHI (5′-CGCGTCATGAATCTGAA-CAAGGATTGAAGTTCTTC-3′) for the SAIL_528_F09 line and AtERD67c +1039f (5′-CAGGTCGTCGGCTTCTGCTT-3′) and AtERD6.7c+1512r (5′-CAG-AGAGGGAGAGAGAGGGTGAC-3′) for the SALK_106049 line.

Nonaqueous Fraction

Unshaded mature rosette leaves were harvested in the middle of the light period and used for subcellular fractionation according to the method described by Krueger et al. (2009). Compartment-specific marker enzymes were used to assign the different gradient fractions to the cytosolic, plastidic, or vacuolar compartment. Activity of the plastid-specific NADP-glyceraldehyde-3-phosphate dehydrogenase (EC 1.1.1.94) was measured according to Stitt et al. (1983), activity of the cytosol-specific uridine diphosphate-Glc pyrophosphorylase (EC 2.7.7.9) was determined as described by Zrenner et al. (1993), and nitrate was used as a vacuolar marker as described (Winter et al., 1994; Cross et al., 2006). Five biological replicates each were done for wild-type and mutant lines. For each biological replicate, data from two technical replicates of marker measurements and from three technical replicates of sugar quantifications via HPAEC-PAD were averaged.

Seed Germination Assay and Quantification of Seed Storage Compounds

For seed germination assays, seeds of both *Aterdl6* mutant lines and the wild type were surface sterilized, and germination was carried out on MS plates containing 2% Glc, 7.2% Glc, 2% Suc, 2% sorbitol, or no sugar. Germination was determined by measuring the time of radicle emergence from triplicate assays with 80 to 140 seeds per plate.

Protein and lipid content of seeds was determined as described (Wingenter et al., 2010). For sugar analysis using HPAEC-PAD, seeds were imbibed for 3 h before ethanol extraction and sugar determination as described.

Sequence data from this article can be found in the GenBank/EMBL data libraries under accession number AY124845.

Supplemental Data

The following materials are available in the online version of this article.

Supplemental Figure S1. Phylogenetic tree of Arabidopsis MSTs and plant ERDL6 orthologs.

Supplemental Figure S2. Tissue- and organ-specific expression patterns of *AtERDL6* (At1g75220) according to the Genevestigator microarray database.

Supplemental Figure S3. Genomic organization of the *AtERDL6* gene and molecular characterization of two independent T-DNA insertion lines for *AtERDL6*.

ACKNOWLEDGMENTS

We thank Silke Oppelt, Rebecca Günther, and Gudrun Steingräber for excellent experimental help and Joshua Der for the provision of unpublished fern sequence data. We thank Khader Awaad for help during the preparation and screening of *BvIMP*-overexpressing lines. We also thank Sabine Strahl for critical reading of the manuscript.

Received September 9, 2011; accepted October 6, 2011; published October 7, 2011.

LITERATURE CITED

Aluri S, Büttner M (2007) Identification and functional expression of the Arabidopsis thaliana vacuolar glucose transporter 1 and its role in seed germination and flowering. Proc Natl Acad Sci USA **104:** 2537–2542

Baena-González E, Rolland F, Thevelein JM, Sheen J (2007) A central integrator of transcription networks in plant stress and energy signalling. Nature **448:** 938–942

Becker D, Kemper E, Schell J, Masterson R (1992) New plant binary vectors with selectable markers located proximal to the left T-DNA border. Plant Mol Biol **20:** 1195–1197

Briskin DP, Thornley WR, Wyse RE (1985) Membrane transport in isolated vesicles from sugarbeet taproot. II. Evidence for a sucrose/H-antiport. Plant Physiol **78:** 871–875

Büttner M (2007) The monosaccharide transporter(-like) gene family in Arabidopsis. FEBS Lett **581:** 2318–2324

Büttner M (2010) The Arabidopsis sugar transporter (AtSTP) family: an update. Plant Biol (Stuttg) (Suppl 1) **12:** 35–41

Chiou TJ, Bush DR (1996) Molecular cloning, immunochemical localization to the vacuole, and expression in transgenic yeast and tobacco of a putative sugar transporter from sugar beet. Plant Physiol **110:** 511–520

Clough SJ, Bent AF (1998) Floral dip: a simplified method for Agrobacterium-mediated transformation of Arabidopsis thaliana. Plant J **16:** 735–743

Conde C, Agasse A, Glissant D, Tavares R, Gerós H, Delrot S (2006) Pathways of glucose regulation of monosaccharide transport in grape cells. Plant Physiol **141:** 1563–1577

Cross JM, von Korff M, Altmann T, Bartzetko L, Sulpice R, Gibon Y, Palacios N, Stitt M (2006) Variation of enzyme activities and metabolite levels in 24 Arabidopsis accessions growing in carbon-limited conditions. Plant Physiol **142:** 1574–1588

Czechowski T, Stitt M, Altmann T, Udvardi MK, Scheible WR (2005) Genome-wide identification and testing of superior reference genes for transcript normalization in Arabidopsis. Plant Physiol **139:** 5–17

Deblaere R, Bytebier B, De Greve H, Deboeck F, Schell J, Van Montagu M, Leemans J (1985) Efficient octopine Ti plasmid-derived vectors for Agrobacterium-mediated gene transfer to plants. Nucleic Acids Res **13:** 4777–4788

Dekkers BJ, Schuurmans JA, Smeekens SC (2004) Glucose delays seed germination in Arabidopsis thaliana. Planta **218:** 579–588

Dinant S, Lemoine R (2010) The phloem pathway: new issues and old debates. C R Biol **333:** 307–319

Doll S, Rodier F, Willenbrink J (1979) Accumulation of sucrose in vacuoles isolated from red beet tissue. Planta **144:** 407–411

Gerhardt R, Heldt HW (1984) Measurement of subcellular metabolite levels in leaves by fractionation of freeze-stopped material in nonaqueous media. Plant Physiol **75:** 542–547

Getz HP (1991) Sucrose transport in tonoplast vesicles of red beet roots is linked to ATP hydrolysis. Planta **185:** 261–268

Getz HP, Klein M (1995) Characteristics of sucrose transport and sucrose-induced H+ transport on the tonoplast of red beet (*Beta vulgaris* L.) storage tissue. Plant Physiol **107:** 459–467

Hanahan D (1983) Studies on transformation of Escherichia coli with plasmids. J Mol Biol **166:** 557–580

Heineke D, Wildenberger K, Sonnewald U, Willmitzer L, Heldt HW (1994) Accumulation of hexoses in leaf vacuoles: studies with transgenic tobacco plants expressing yeast-derived invertase in the cytosol, vacuole or apoplasm. Planta **194:** 29–33

Holsters M, Silva B, Van Vliet F, Genetello C, De Block M, Dhaese P, Depicker A, Inzé D, Engler G, Villarroel R, et al (1980) The functional organization of the nopaline A. tumefaciens plasmid pTiC58. Plasmid **3:** 212–230

Hummel J, Niemann M, Wienkoop S, Schulze W, Steinhauser D, Selbig J, Walther D, Weckwerth W (2007) ProMEX: a mass spectral reference database for proteins and protein phosphorylation sites. BMC Bioinformatics **8:** 216

Ingram J, Bartels D (1996) The molecular basis of dehydration tolerance in plants. Annu Rev Plant Physiol Plant Mol Biol **47:** 377–403

Jaquinod M, Villiers F, Kieffer-Jaquinod S, Hugouvieux V, Bruley C, Garin J, Bourguignon J (2007) A proteomics dissection of Arabidopsis thaliana vacuoles isolated from cell culture. Mol Cell Proteomics **6:** 394–412

Kaplan F, Kopka J, Haskell DW, Zhao W, Schiller KC, Gatzke N, Sung DY, Guy CL (2004) Exploring the temperature-stress metabolome of Arabidopsis. Plant Physiol **136:** 4159–4168

Karimi M, Inzé D, Depicker A (2002) GATEWAY vectors for Agrobacterium-mediated plant transformation. Trends Plant Sci **7:** 193–195

Karrer EE, Rodriguez RL (1992) Metabolic regulation of rice alpha-amylase and sucrose synthase genes in planta. Plant J **2:** 517–523

Keller F (1992) Transport of stachyose and sucrose by vacuoles of Japanese artichoke (*Stachys sieboldii*) tubers. Plant Physiol **98:** 442–445

Kiyosue T, Abe H, Yamaguchi-Shinozaki K, Shinozaki K (1998) ERD6, a cDNA clone for an early dehydration-induced gene of Arabidopsis, encodes a putative sugar transporter. Biochim Biophys Acta **1370:** 187–191

Krueger S, Niehl A, Lopez Martin MC, Steinhauser D, Donath A, Hildebrandt T, Romero LC, Hoefgen R, Gotor C, Hesse H (2009) Analysis of cytosolic and plastidic serine acetyltransferase mutants and subcellular metabolite distributions suggests interplay of the cellular compartments for cysteine biosynthesis in Arabidopsis. Plant Cell Environ **32:** 349–367

Li Y, Lee KK, Walsh S, Smith C, Hadingham S, Sorefan K, Cawley G, Bevan MW (2006) Establishing glucose- and ABA-regulated transcription networks in Arabidopsis by microarray analysis and promoter classification using a Relevance Vector Machine. Genome Res **16:** 414–427

Livak KJ, Schmittgen TD (2001) Analysis of relative gene expression data using real-time quantitative PCR and the $2^{-\Delta\Delta C_T}$ method. Methods **25:** 402–408

Lloyd JC, Zakhleniuk OV (2004) Responses of primary and secondary metabolism to sugar accumulation revealed by microarray expression analysis of the Arabidopsis mutant, pho3. J Exp Bot **55:** 1221–1230

Martinoia E, Kaiser G, Schramm MJ, Heber U (1987) Sugar transport across the plasmalemma and the tonoplast of barley mesophyll protoplasts: evidence for different transport systems. J Plant Physiol **131:** 467–478

Martinoia E, Maeshima M, Neuhaus HE (2007) Vacuolar transporters and their essential role in plant metabolism. J Exp Bot **58:** 83–102

Martinoia E, Massonneau A, Frangne N (2000) Transport processes of solutes across the vacuolar membrane of higher plants. Plant Cell Physiol **41:** 1175–1186

Pollock CJ, Farrar J, Koroleva OA, Gallagher JA, Tomos AD (2000) Intracellular and intercellular compartmentation of carbohydrate metabolism in leaves of temperate Gramineae. Rev Bras Bot **23:** 349–357

Poschet G, Hannich B, Büttner M (2010) Identification and characterization of AtSTP14, a novel galactose transporter from Arabidopsis. Plant Cell Physiol **51:** 1571–1580

Price J, Laxmi A, St Martin SK, Jang JC (2004) Global transcription profiling reveals multiple sugar signal transduction mechanisms in *Arabidopsis*. Plant Cell **16:** 2128–2150

Price J, Li TC, Kang SG, Na JK, Jang JC (2003) Mechanisms of glucose signaling during germination of Arabidopsis. Plant Physiol **132:** 1424–1438

Rausch T (1991) The hexose transporters at the plasma membrane and the tonoplast of higher plants. Physiol Plant **82:** 134–142

Ristic Z, Ashworth EN (1993) Changes in leaf ultrastructure and carbohydrates in *Arabidopsis thaliana* L. (Heyn) cv. Columbia during rapid cold acclimation. Protoplasma **172:** 111–123

Roberts MR, de Bruxelles GL (2001) Signals regulating multiple responses to wounding and herbivores. Crit Rev Plant Sci **20:** 487–521

Ruan YL, Jin Y, Yang YJ, Li GJ, Boyer JS (2010) Sugar input, metabolism, and signaling mediated by invertase: roles in development, yield potential, and response to drought and heat. Mol Plant **3:** 942–955

Sauer N (2007) Molecular physiology of higher plant sucrose transporters. FEBS Lett **581:** 2309–2317

Schneidereit A, Scholz-Starke J, Büttner M (2003) Functional characterization and expression analyses of the glucose-specific AtSTP9 monosaccharide transporter in pollen of Arabidopsis. Plant Physiol **133:** 182–190

Sherson SM, Alford HL, Forbes SM, Wallace G, Smith SM (2003) Roles of cell-wall invertases and monosaccharide transporters in the growth and development of Arabidopsis. J Exp Bot **54:** 525–531

Shulaev V, Cortes D, Miller G, Mittler R (2008) Metabolomics for plant stress response. Physiol Plant **132:** 199–208

Stitt M, Wirtz W, Heldt HW (1983) Regulation of sucrose synthesis by cytoplasmic fructosebisphosphatase and sucrose phosphate synthase during photosynthesis in varying light and carbon dioxide. Plant Physiol **72:** 767–774

Thom M, Komor E (1984) H^+-sugar antiport as the mechanism of sugar uptake by sugarcane vacuoles. FEBS Lett **173:** 1–4

Thom M, Komor E, Maretzki A (1982) Vacuoles from sugarcane suspension cultures. II. Characterization of sugar uptake. Plant Physiol **69:** 1320–1325

Tilsner J, Kassner N, Struck C, Lohaus G (2005) Amino acid contents and transport in oilseed rape (Brassica napus L.) under different nitrogen conditions. Planta **221:** 328–338

To JP, Reiter WD, Gibson SI (2002) Mobilization of seed storage lipid by Arabidopsis seedlings is retarded in the presence of exogenous sugars. BMC Plant Biol **2:** 4

Voitsekhovskaja OV, Koroleva OA, Batashev DR, Knop C, Tomos AD, Gamalei YV, Heldt HW, Lohaus G (2006) Phloem loading in two Scrophulariaceae species: what can drive symplastic flow via plasmodesmata? Plant Physiol **140:** 383–395

Wagner GJ (1979) Content and vacuole/extravacuole distribution of neutral sugars, free amino acids, and anthocyanin in protoplasts. Plant Physiol **64:** 88–93

Williams LE, Lemoine R, Sauer N (2000) Sugar transporters in higher plants: a diversity of roles and complex regulation. Trends Plant Sci **5:** 283–290

Wingenter K, Schulz A, Wormit A, Wic S, Trentmann O, Hoermiller II, Heyer AG, Marten I, Hedrich R, Neuhaus HE (2010) Increased activity of the vacuolar monosaccharide transporter TMT1 alters cellular sugar partitioning, sugar signaling, and seed yield in Arabidopsis. Plant Physiol **154:** 665–677

Wingenter K, Trentmann O, Winschuh I, Hörmiller II, Heyer AG, Reinders J, Schulz A, Geiger D, Hedrich R, Neuhaus HE (2011) A member of the mitogen-activated protein 3-kinase family is involved in the regulation of plant vacuolar glucose uptake. Plant J **68:** 129–136

Winter H, Robinson D, Heldt H (1994) Subcellular volumes and metabolite concentrations in spinach leaves. Planta **193:** 530–535

Wormit A, Trentmann O, Feifer I, Lohr C, Tjaden J, Meyer S, Schmidt U, Martinoia E, Neuhaus HE (2006) Molecular identification and physiological characterization of a novel monosaccharide transporter from *Arabidopsis* involved in vacuolar sugar transport. Plant Cell **18:** 3476–3490

Yamada K, Osakabe Y, Mizoi J, Nakashima K, Fujita Y, Shinozaki K, Yamaguchi-Shinozaki K (2010) Functional analysis of an Arabidopsis thaliana abiotic stress-inducible facilitated diffusion transporter for monosaccharides. J Biol Chem **285:** 1138–1146

Zeeman SC, Smith SM, Smith AM (2007) The diurnal metabolism of leaf starch. Biochem J **401:** 13–28

Zrenner R, Willmitzer L, Sonnewald U (1993) Analysis of the expression of potato uridinediphosphate-glucose pyrophosphorylase and its inhibition by antisense RNA. Planta **190:** 247–252